Liquid Phase Epitaxy (LPE) Formation of Localized High Quality and Mobility Ge & SiGe by High Dose Ge-Implantation with Laser Melt Annealing for 10nm and 7nm Node CMOS Technology

John Borland[1,2], Michiro Sugitani[3], Peter Oesterlin[4], Walt Johnson[5], Temel Buyuklimanli[6], Robert Hengstebeck[6] , Ethan Kennon[7], Kevin Jones[7] & Abhijeet Joshi[8]

[1]JOB Technologies, Aiea, Hawaii
[2]AIP, Honolulu, Hawaii
[3]SEN, Shinagawa, Tokyo, Japan
[4]Innovavent, Gottingen, Germany
[5]KLA-Tencor, Milpitas, California
[6]EAG, East Windsor, New Jersey
[7]University of Florida, Gainesville, FL
[8]Active Layer Parametrics, Los Angeles, CA

We investigated using high dose (5E16/cm^2) Ge beam-line ion implantation in combination with laser melt annealing as an alternative to Ge-epi by CVD to form high quality single crystal Ge-epilayer by LPE (liquid phase epitaxy) that is very uniform, thin 10-25nm and localized for high mobility Ge-channels. The implant resulted in 7nm amorphous Ge deposition by a method called dose controlled deposition (DCD). A 515nm laser was used to vary the melt depth from 9nm to 500nm based on laser anneal pulse duration and power level. Ellipsometer was used to measure the surface amorphous layer thickness while therma-wave (TW) analysis was used to monitor Ge implant damage recovery after LPE. SIMS depth profiles showed Ge surface concentration varied from 100% down to 2% based on the laser melt depth. X-TEM analysis showed the transformation of deposited amorphous Ge surface layer to single crystal Ge after laser melt and LPE. Sb implantation at two dose levels of 3E15/cm^2 and 3E13/cm^2 was used to examine laser melt annealing effects on n-type dopant activation and electron mobility in Ge. Special Hx-probe tips on the 4PP system was required to measure sheet resistance and CAOT/DHE method was used for Differential Hall Effect measurements.

Introduction

Localized Ge and SiGe high quality surface material region on bulk-Si and SOI wafers are needed for 10nm and 7nm node CMOS technology. Traditionally SiGe and Ge surface layers on bulk-Si or SOI wafers are realized by Chemical Vapor Deposition (CVD) or Vapor Phase Epi (VPE) epitaxial growth at elevated temperatures (400^{o}C to 800^{o}C) and Ge selective epitaxial growth (SEG) can be achieved with an oxide hard mask. To reduce defects strain relaxed buffer (SRB) or aspect ratio trapping (ART) have been employed with Ge-epi on bulk-Si while others have used Ge layer transfer wafer bonding

techniques for GeOI or SiGeOI. One issue with Ge-epi growth by CVD is poor uniformity especially for thin layers 5-50nm thick and for selective epi it can be much worse due to pattern density local loading effects and nucleation delay time from surface impurities within the small oxide mask windows, ion implantation on the other hand has extremely tight uniformity of 0.2-0.5%. An alternative to Ge-epi by CVD or VPE is to use either SPE (solid phase epitaxy) or LPE (liquid phase epitaxy) to form high quality single crystal Ge or SiGe epitaxial surface layers from an amorphous Ge layer using the Si substrate wafer as a seed layer for single crystal epitaxial regrowth. SPE annealing technique is commonly used with ion implantation when the implant dose is high enough to cause sufficient surface damage to amorphize it. Ge species is typical used to amorphize the surface region of Si when the dose is >5E14/cm^2 to depths from as shallow as 5nm (3keV) to 60nm (40keV) as reported by Borland at IEEE RTP-2009 and shown in Fig.1 below for Ge, Si, In, Sb and Xe implant species dose and energy on surface amorphous layer depth into Si (100) wafers (1).

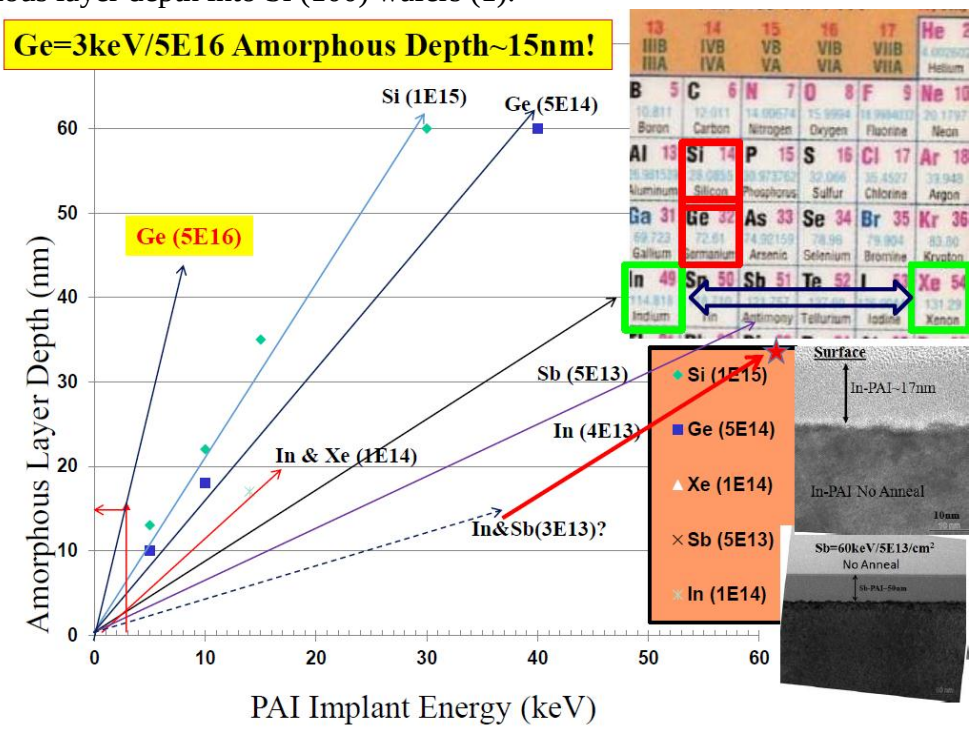

Fig.1: Comparison of various implant species energy and dose on surface amorphous layer depth.

Using high dose >E16/cm^2 Ge-infusion doping by Gas Cluster Ion Beam (GCIB) technique with photoresist soft mask was proposed in 2004 by Borland et al. resulting in localized amorphous Ge surface deposition 33-70nm thick by dose control deposition with a reported uniformity of 0.52% on 300mm wafers (2,3,4). They reported using low temperature SPE to form single crystal Ge epitaxial layers but residual Ge implant end-of-range (EOR) damage remained beyond the amorphous crystalline interface. Using PR (photoresist) soft masking technique with high-k/metal gate last approach, localized high mobility Ge-channels could be formed by Ge doping directly into the channel region thereby leaving the n+ S/D regions composed of Si material for high n+ dopant activation and shallow junction formation avoiding enhanced diffusion of n-type dopant in Ge as others have reported (3). This proposal by Borland is shown in Fig.2a below (3). Today, the industry has moved from planar 2-D devices to 3-D FinFET devices requiring a

change to the original proposal as shown in Fig. 2b where the Ge or SiGe Fin region is first formed then the n+S/D region is recess etched away and Si-SEG is selectively grown and then doped n+ by implantation leaving just Ge in the channel/Fin region. High n+ dopant activation in the n+Si S/D region is realized with minimal dopant diffusion similar to a Si-capping layer on Ge as reported by Borland & Konkola at IIT-2014 and reduced Ge-epi threading dislocation (5).

Laser melt annealing of implanted junctions are currently being used in production for high quality back-side illuminated CMOS image sensors used in smart phone cameras by several IC and foundry semiconductor manufacturers and if the melt depth exceeds the implant damage depth complete elimination of all residual implant damage/defects occurs with 100% dopant activation (6). Last year at IWJT-2013 Borland et al. (7) reported using Ge-plasma ion implantation at 1E16/cm^2 and 1E17/cm^2 doses with selective/localized laser melt annealing to realize high quality up to 55% Ge epilayer by LPE with >4x higher hole mobility (160cm^2/Vs) due to the high Ge surface level and surface strain without residual implant damage or end-of-range defects when the laser melt depth exceeded the amorphous Ge implant depth which was 60nm. One limitation they noted with plasma Ge implantation was poor retained Ge dose due to surface sputtering at low energies which limited the Ge content to 55% for the 1E17/cm^2 dose so 100% surface Ge by DCD could not be realized with plasma Ge implantation, 1E16/cm^2 Ge dose achieved 20% Ge (7). Therefore to overcome this retained dose problem we investigated Ge beam-line ion implantation in this study to achieve higher retained dose for precise controlled Ge deposition by DCD at 5E16/cm^2 Ge implant dose.

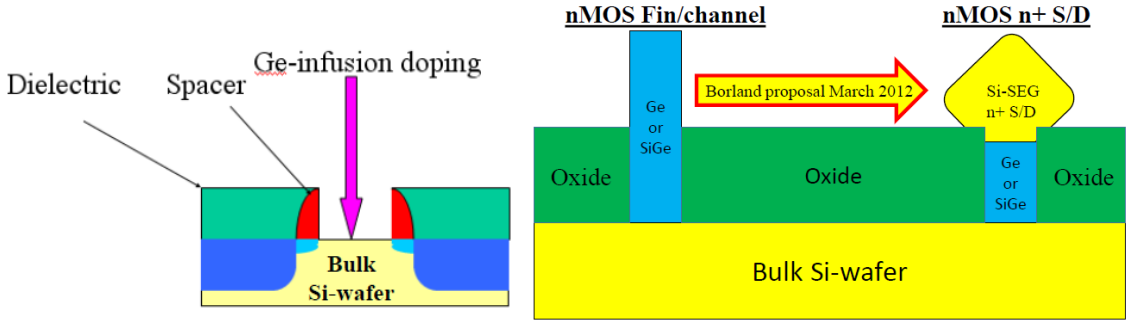

(a) (b)

Fig.2: a) Planar Ge nMOS using Ge channel formation by gate last approach, b) nMOS Ge-FinFET were Ge Fin/channel and Si-epi for n+S/D region.

Experimentation

300mm P(100) wafers were first implanted with Sb at 3keV energy and either 3E15/cm^2 or 3E13/cm^2 dose to compare E20/cm^3 n+ S/D doping levels to E18/cm^3 channel doping levels on dopant activation in Ge or Si material and the effects it would have on electron mobility. The notch half of each wafer was then implanted with Ge species at 3keV energy and 5E16/cm^2 dose to achieve a thin deposited surface amorphous Ge layer by DCD. Using ellipsometry measurements, we verified the surface amorphous Ge layer thickness/depth was 14.7nm while the Sb 3E15/cm^2 region amorphous Si layer measured 6.2nm. From Fig.1 the Sb 3keV 3E13/cm^2 amorphous layer would be in the noise level of the native oxide at <2nm. The therma-wave (TW) implant damage value for just the Sb=3keV/3E15 implant was TW=1126 while for Sb+Ge implant TW=2816.

The lower Sb dose Sb=3keV/3E13 implant TW=697 and Sb+Ge implant TW=2353. So the added contribution for the Ge=3keV/5E16 implant on TW was +1673 (TW is an arbitrary unit).

After implant the 2 wafers were sent to Innovavent in Gottingen, Germany for laser annealing using their 515nm laser. To vary the melt depth we selected 3 different pulse duration laser anneal times of 300ns, 600ns and 1200ns. For the 300ns anneal time we selected 5 different power levels of 0.2, 0.4, 0.8, 1.6 and 3.2 J/cm^2 while for the 600ns and 1200ns anneal times we selected 0.25, 0.5, 1.0, 2.0 and 4.0 J/cm^2 power levels. The laser anneal pattern is shown below in Fig.3, the 200mm line scans are 10.4mm wide with 1mm spacing and 6mm spacing between the 3 groups of anneals. The notch half of the wafers received the half wafer high dose Ge implant so each laser line scan pattern anneal, anneals both the Ge+Sb implant bottom half of the wafer and the Sb only top half of the wafer allowing metrology line scans through the various laser anneal conditions.

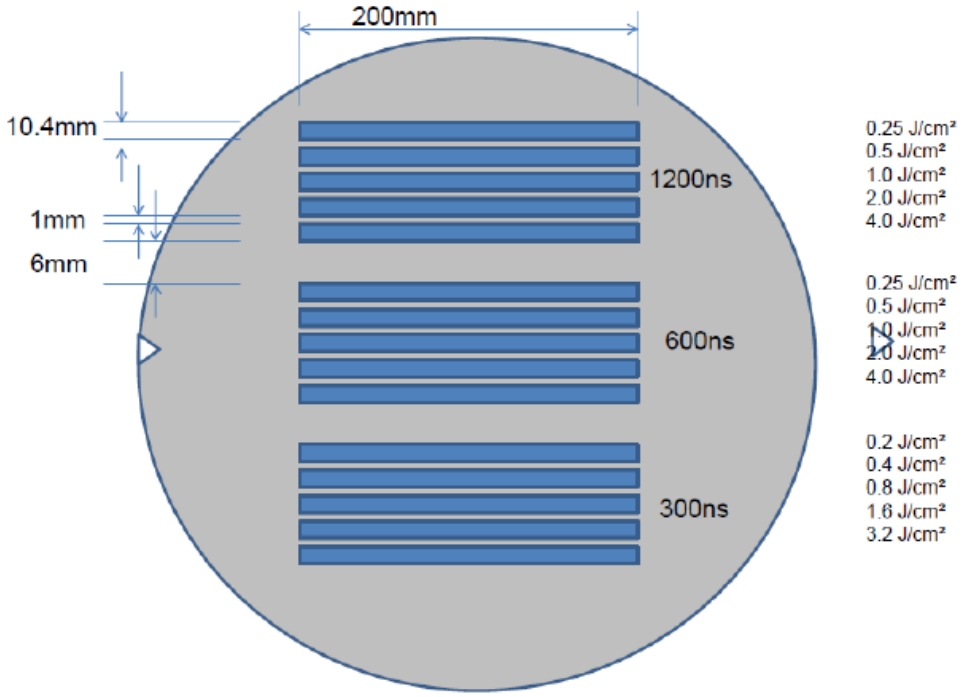

Fig.3: Line scan laser anneal pattern on each wafer.

Results

Ellipsometry Amorphous Layer Thickness

Ellipsometry line scan measurements were used to determine the amorphous layer thickness before and after laser annealing of the Sb only implanted region of 3E15/cm^2 and the Sb+Ge implanted region (Ge=5E16/cm^2) as shown below in Fig.4. Fig.4 a & b are for the Sb only implanted regions while Fig.4 c, d & e are for the Sb+Ge co-implanted regions. Fig.4a shows the line scan for Sb only with 300ns anneal time at 3.2J, 1.6J, 0.8J, 0.4J and 0.2J laser anneal power levels. The amorphous layer thickness was 6.3nm in the unannealed regions on the left and right sides of the line scans and stays at 6.3nm for the 0.2J and 0.4J anneals but drops to 5.7nm for the 0.8J anneal then to 0.5nm for the 1.6J anneal and finally to 0.0nm for the 3.2J anneal region signifying complete laser melt annealing with no remaining surface native oxide. The 600ns anneal results

are shown in Fig.4b, this time the 1J anneal region was 5.9nm, 2J was 1.1nm and 4J was 0.0nm. Adding the Ge implant increased the surface amorphous layer thickness to 14.7nm or +8.4nm. Fig.4c shows the 300ns anneal region with no change for the 0.2J and 0.4J anneals but with 0.8J it drops to 14.1nm, 1.6J anneal to 7.5nm and 3.2J anneal to 0.5nm. Increasing the anneal time to 600ns had little effects as shown in Fig.4d but the 1200ns anneal time results were quite different as shown in Fig.4e. At 1200ns/2J the amorphous layer thickness dropped to 13.5nm and at 1200ns/4J to 9.3nm suggesting much shallower melt depths and therefore incomplete Ge LPE. As will be shown later the after anneal ellipsometry amorphous layer thickness are not supported by the SIMS melt depth profiles and X-TEM images which will show complete Ge-LPE with some residual implant defects.

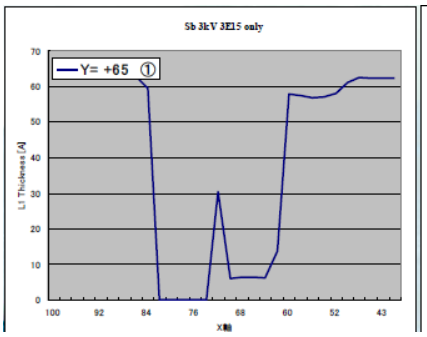

(a) 300ns Sb

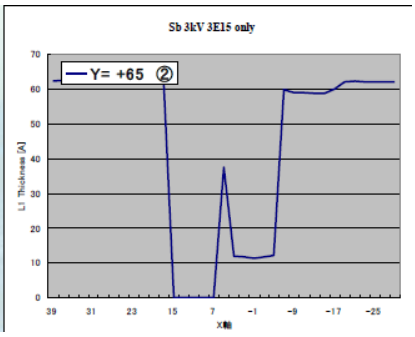

(b) 600ns Sb

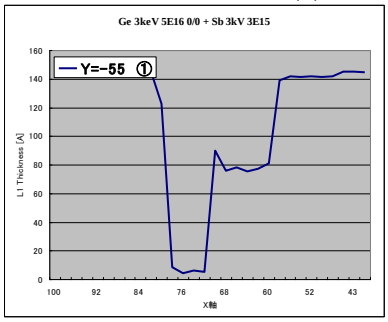

(c) 300ns Ge+Sb

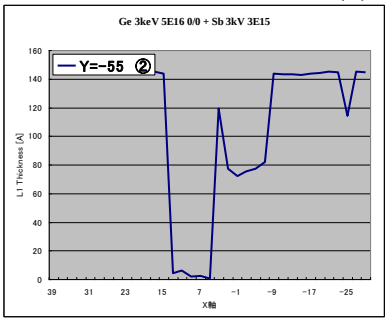

(d) 600ns Ge+Sb

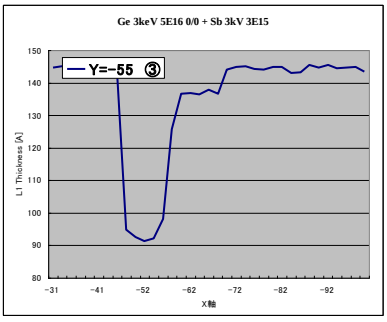

(e) 1200ns Ge+Sb

Fig.4: Ellipsometry measurements of the Sb and Sb+Ge amorphous layer thickness after various laser annealing conditions.

Therma-Wave Implant and After Anneal Damage Analysis

TW wafer map with corresponding line scans are shown in Fig.5 a & b for the Sb=3E15/cm^2 full wafer and Ge=5E16/cm^2 half wafer implants and this characterization technique clearly shows the effectiveness of the laser anneal parameters on Ge and Sb LPE and any residual implant damage. All 5 laser annealing power levels can only be detected for the Ge implanted region using the 300ns anneal time, the other 600ns and 1200ns cases show only 3 and 2 laser annealing scans respectively in Fig.5a for laser power level of 4J , 2J and 1J. Fig.6 shows the TW wafer map and TW line scans for the Sb=3E13/cm^2 full wafer and Ge=5E16/cm^2 half wafer implants. Complete implant damage recovery occurs at lower laser anneal power levels. The detailed TW results for all the implanted and laser annealing conditions are plotted in Fig.7 for TW versus laser power. Complete implant annealing and damage recovery by LPE is realized when the TW value saturates, for the Sb=3E13/cm^2 region this is when TW is <500, for Sb=3E15/cm^2 region this is when TW is <750 and for the Ge=5E16/cm^2 region this is when TW is <1200. At the longer laser anneal pulse duration times much higher laser

power is required for TW saturation and LPE for complete implant damage recovery. Fig. 7 shows that for the low and high dose Sb implant complete LPE occurs for 300ns when power level is >1.6J, for 600ns and 1200ns at >2J. Adding Ge implant to the low dose Sb did not change the 300ns and 600ns anneal, LPE at >1.6J but the 1200ns anneal required >4J for LPE. Ge with the high dose Sb requires >3.2J power for the 300ns anneal and >4J for the 600ns anneal but the 1200ns anneal did not achieve complete LPE leaving residual implant damage and TW=1700.

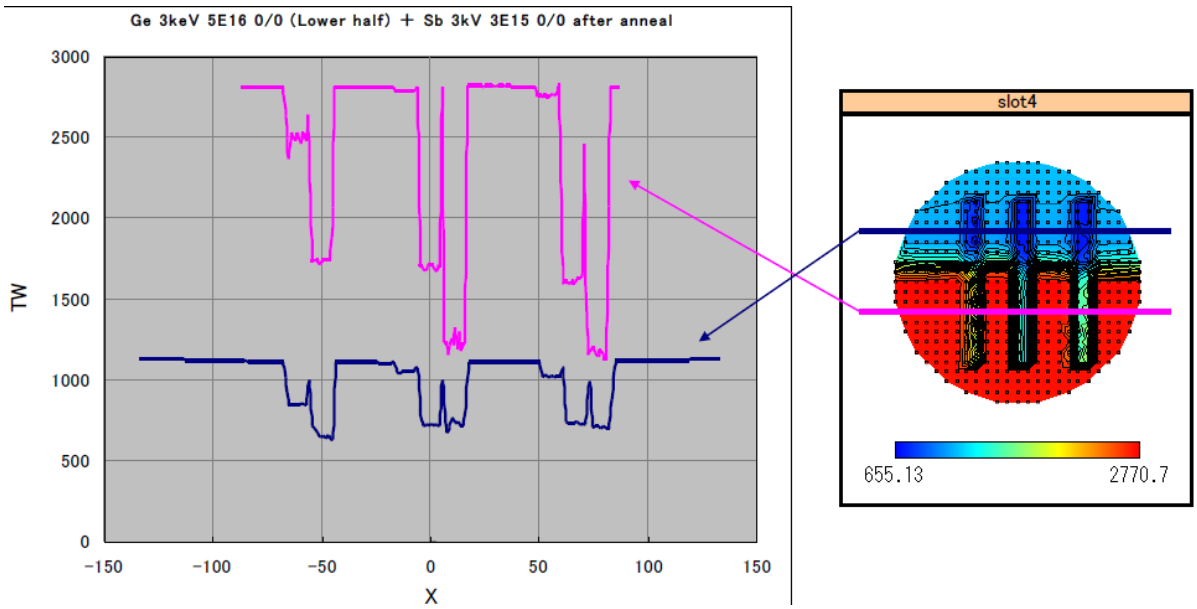

(a)Line scan (b) Wafer map

Fig.5: Therma-wave results for the Sb=3E15/cm^2 and Ge=5E16/cm^2 implanted wafer.

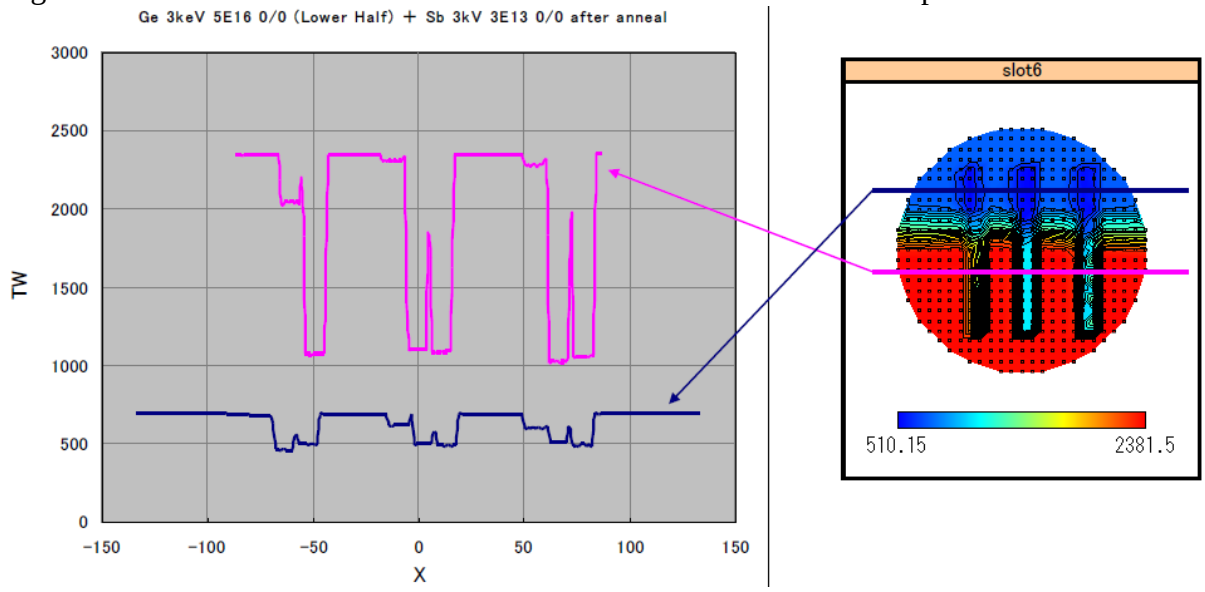

(a) Line scan (b) Wafer map

Fig.6: Therma-wave results for the Sb=3E13/cm^2 and Ge=5E16/cm^2 implanted wafer.

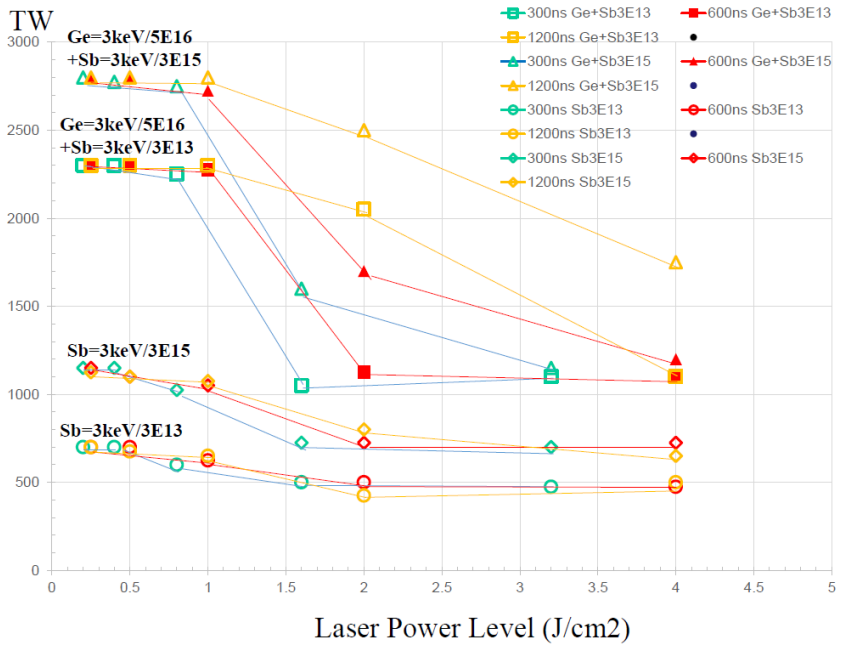

Fig.7: Therma-wave results of residual Ge-implant damage after various LPE laser melt

Dopant Activation Sheet Resistance Measurements by 4PP with Hx-Probes

Highest laser anneal power and shortest pulse duration anneal times were needed to achieve complete dopant activation of Sb implants for the Sb=3E15/cm^2 and Ge=5E16/cm^2 co-implant conditions to achieve Rs=33Ω/□ as shown in Fig.8 for the Rs line scans and Fig.9 for the Rs versus laser power plot. At the lower laser anneal power levels the Rs values on the Sb+Ge regions are about 10x higher when compared to the Sb only region. This may be due to the much shallower Sb junction (x_j) and melt depth as will be discussed and shown later in Fig.13. With standard RTA annealing at 1050ºC/10sec the best Rs achieved was only 700Ω/□ so a 21x improvement in Sb activation level is realized with laser melt annealing. Dopant activation requires considerable more laser power than that required for implant damage recovery when we compare the start of TW saturation level in Figs. 5,6&7 to the start of Rs saturation level in Figs. 8&9. Fig.10 below shows the 4PP Rs line scans for the Sb=3E13/cm^2 were Rs=1000Ω/□ for full dopant activation. Note again that for the lower laser anneal power levels 4PP Rs values could not be measured on the Sb+Ge co-implant regions except for the 300ns/3.2J and 600ns/4J anneal conditions.

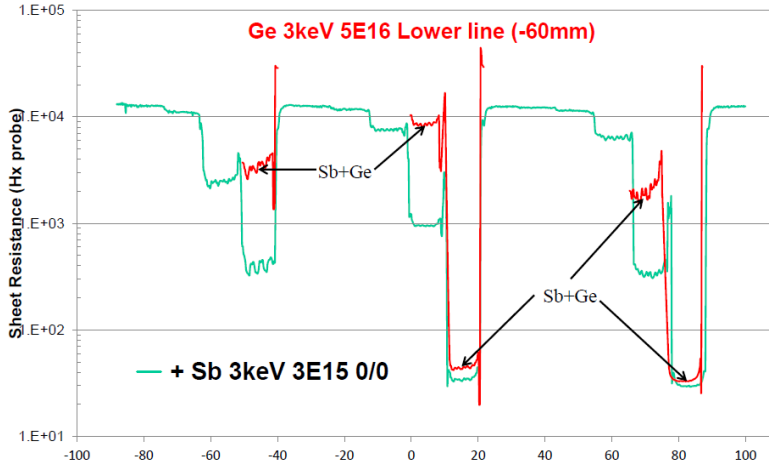

Fig.8: Line scan 4PP Rs measurements using Hx-probe for the Ge+Sb (3E15).

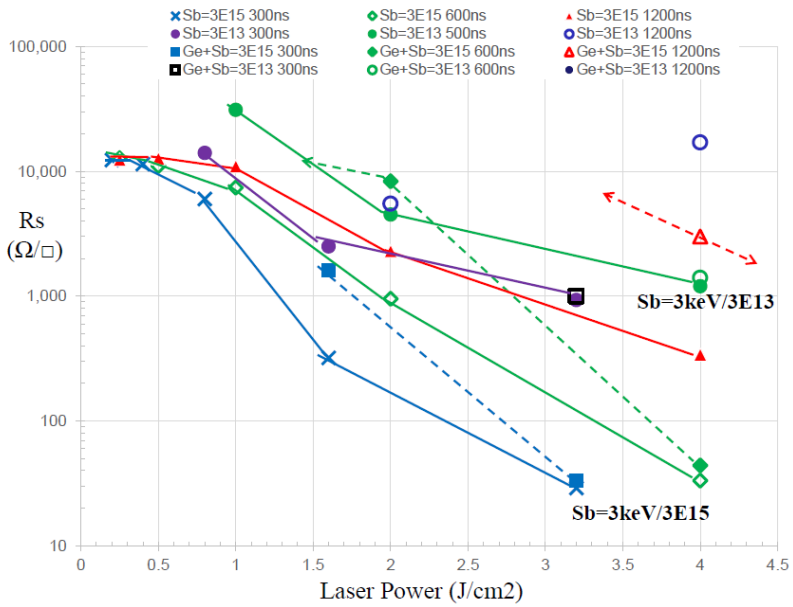

Fig.9: Plot of Rs versus laser power for the various implant conditions.

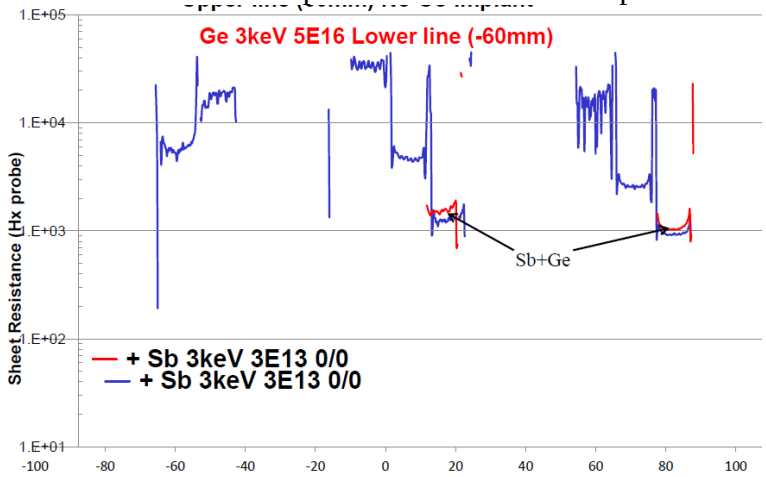

Fig.10: Line scan 4PP Rs measurements using Hx-probe for the Ge+Sb (3E13).

<u>SIMS Chemical Depth Profiles and X-TEM Analysis to Determine Ge LPE Melt Depth amd Crystal Quality</u>

SIMS profile of the unannealed region for the Sb(3E15)+Ge(5E16) is shown in Fig.11 showing the Si, Ge, Sb and O chemical depth profiles. A thin surface GeSiO layer <1.7nm is detected followed by a 7.0nm thick deposited amorphous Ge-layer with Ge areal density of 4.4E16/cm^2 that transistions to a 7% amorphous SiGe region 14.7nm deep. The Sb peak is 2.5E22/cm^3 (areal density of 8.8E15/cm^2) with a junction depth (x_j) of 12.5nm at 5E18/cm^3. The surface oxide O depth profile shows the surface native oxide knock-in effect caused by the Ge implant with an O areal density of 7.4E15/cm^2. Fig.12 shows the X-TEM micrographs of the Sb+Ge unannealed SIMS region from Fig.11. The total Ge amorphous depth is 14.7nm and the bright white band at the Ge/Si interface is the 3nm amorphous SiGe transistion region from 50% Ge to 7% Ge. Below the 7% Ge is the crystalline Si wafer. With the 1200ns laser anneal at 4J/cm^2 the Ge implant half of the wafer had a melt depth of 25nm reducing the Ge surface level to 95% and Sb x_j of 25nm as shown in the SIMS profile comparing it to the control unannealed region in Fig.13. The Sb only region without Ge implant melt depth was much deeper,

70nm with an Sb x_j of 60.5nm as shown by the SIMS profile in Fig.13. The 515nm laser melt depth is know to be shallower with deeper surface amorphous layers and from the Rs results in Figs.8&14 the electrically activated dose for the 3000Ω/□ shallow Sb junction at 25nm is 1E13/cm^2 (Sb areal density of 5.5E15/cm^2) while for the deeper 60.5nm Sb junction with Rs=400Ω/□ the electrically activated dose is 1E14/cm^2 (Sb areal density of 2.9E15/cm^2). Fig.14 is a plot of Rs versus P or Sb implant dose with laser and RTA annealing (5,8). Laser melt annealing can achieve 100% Sb dopant activation for the deeper anneals while RTA is limited to <5% for the high dose and 50% at the low dose shown in Fig.14. The solid solubility of Sb in Si is 6.8E19/cm^3 so the shallow Sb junctions in Fig.13 contains considerable amount of chemical, electrically inactive Sb, about 1 in 300 active Sb atoms in the 25nm junction while 1 in 30 Sb atoms in the 60.5nm junction. X-TEM of the 1200ns/4J Sb+Ge sample is Fig.13 is shown in Fig.15 with a Ge melt depth of 25nm and TW value of 1700 so still some residual implant damage and not the 9.3nm amorphous layer measured by ellipsometry in Fig.4e. The next X-TEM in Fig.16 is for the 300ns/1.6J case with a melt depth of <10nm and Ge-polycrystalline with a TW of also 1600, Fig.4c ellipsometry measured 7.5nm amorphous layer. The deepest laser melt condition was 300ns and 3.2J/cm^2 power level as shown in Fig.17 SIMS results. The Ge region had a melt depth of 420nm with Sb x_j at 370nm and Ge-LPE level of 7% while the region without Ge, melt depth was 490nm with Sb x_j at 420nm. The Rs for both regions was 33Ω/□ as shown in Figs.8&9 corresponding to 100% Sb dopant activation in Fig.14.

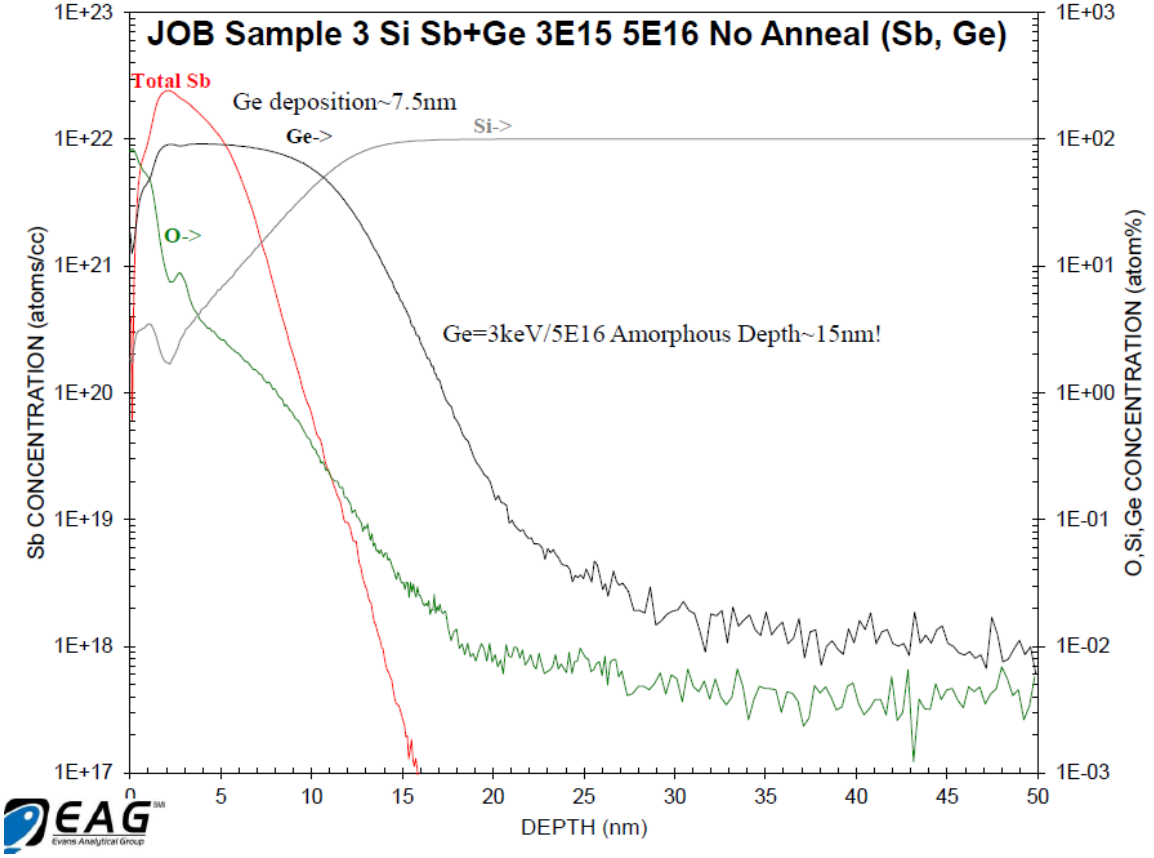

Fig.11: No annealed Sb(3E15)+Ge(5E16) region showing 100% Ge deposition 7.5nm thick and Sb peak 2.5E22/cm^3.

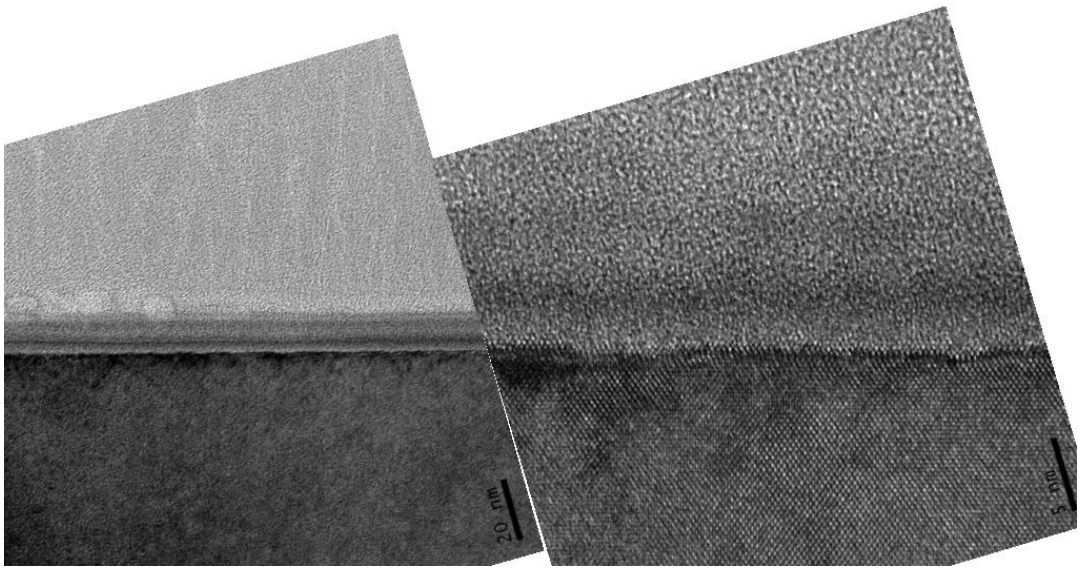

Fig.12: X-TEM of the Ge+Sb (3E15) unannealed region with a Ge amorphous layer depth of 14.7nm and TW value of 1800.

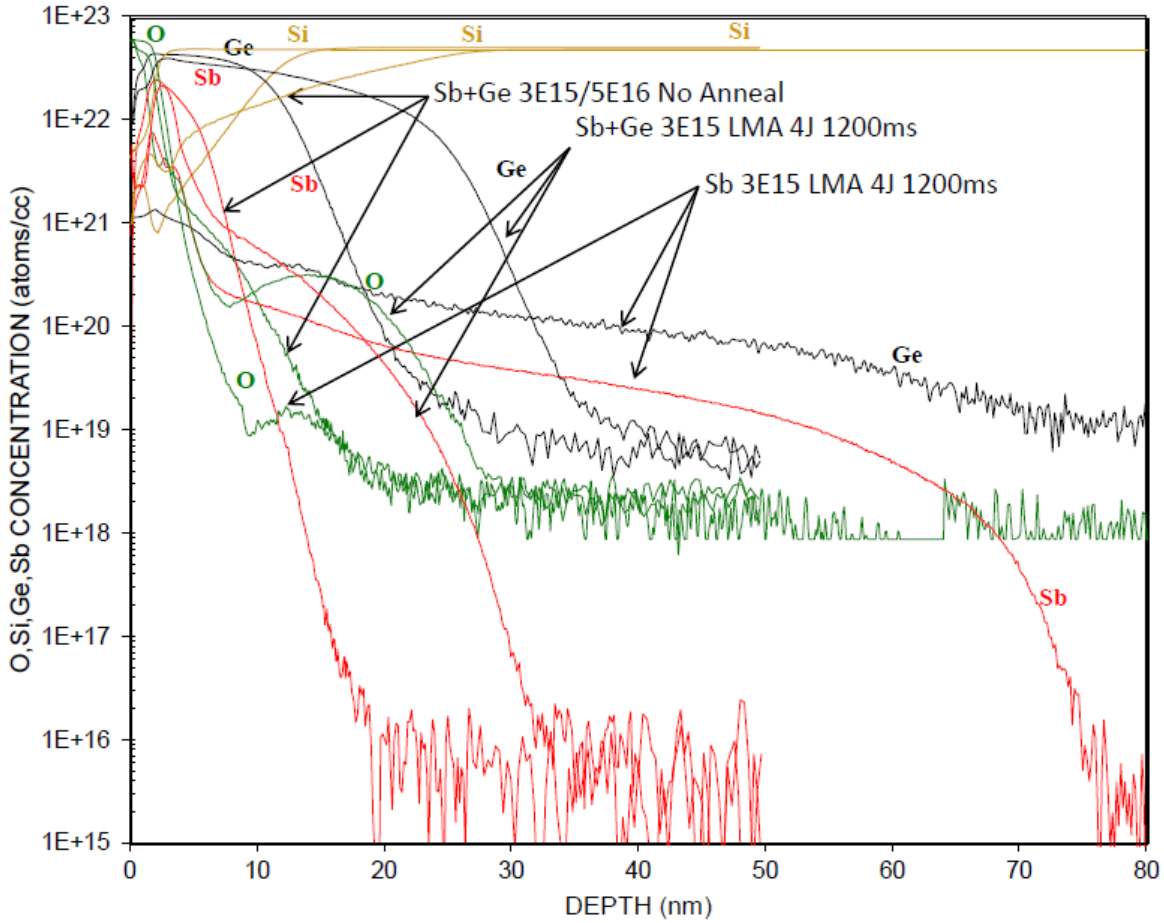

Fig.13: SIMS profie comparison for 1200ns laser anneal at 4J, Ge+Sb region melt depth of 25nm while Sb only region melt depth of 65nm.

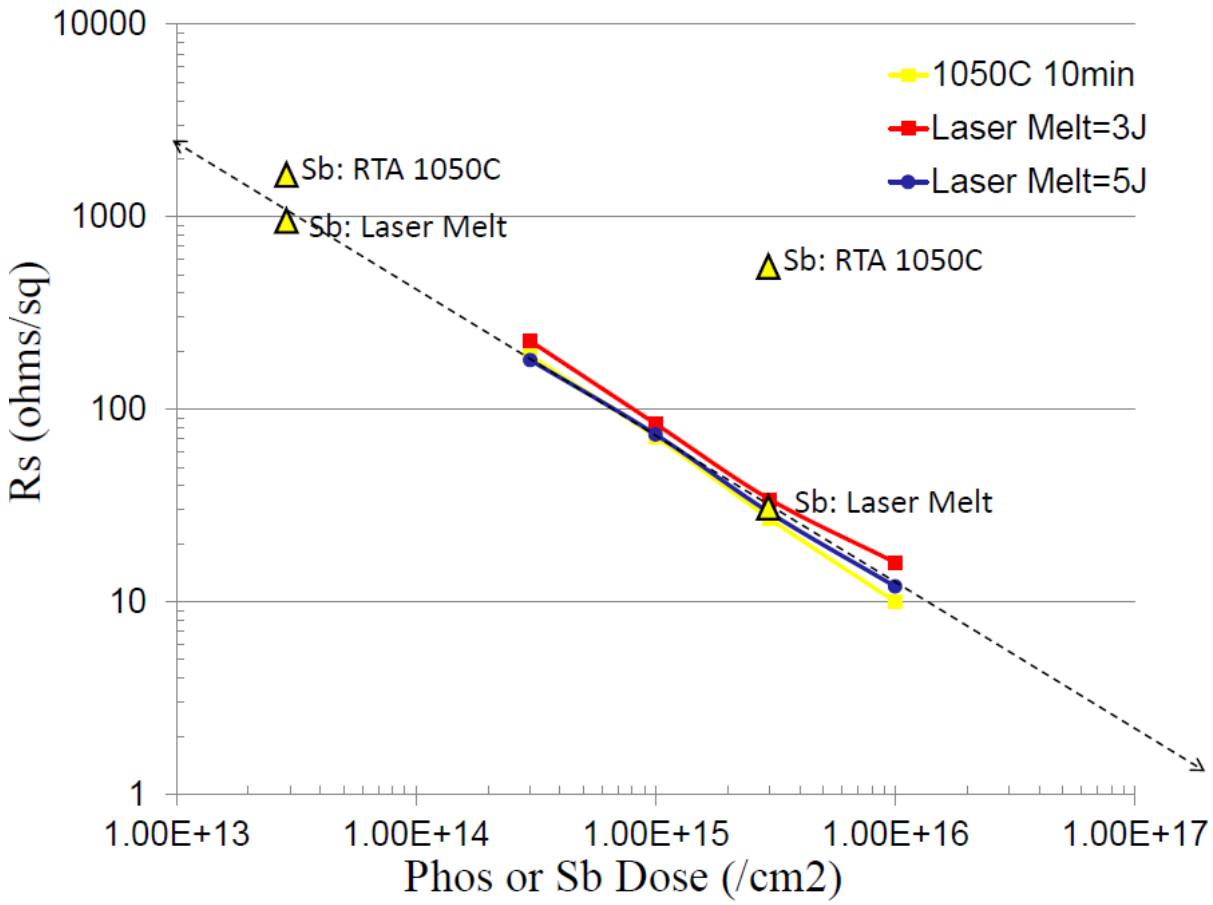

Fig.14: Rs versus P or Sb implant dose for various laser and RTA anneals (5,8).

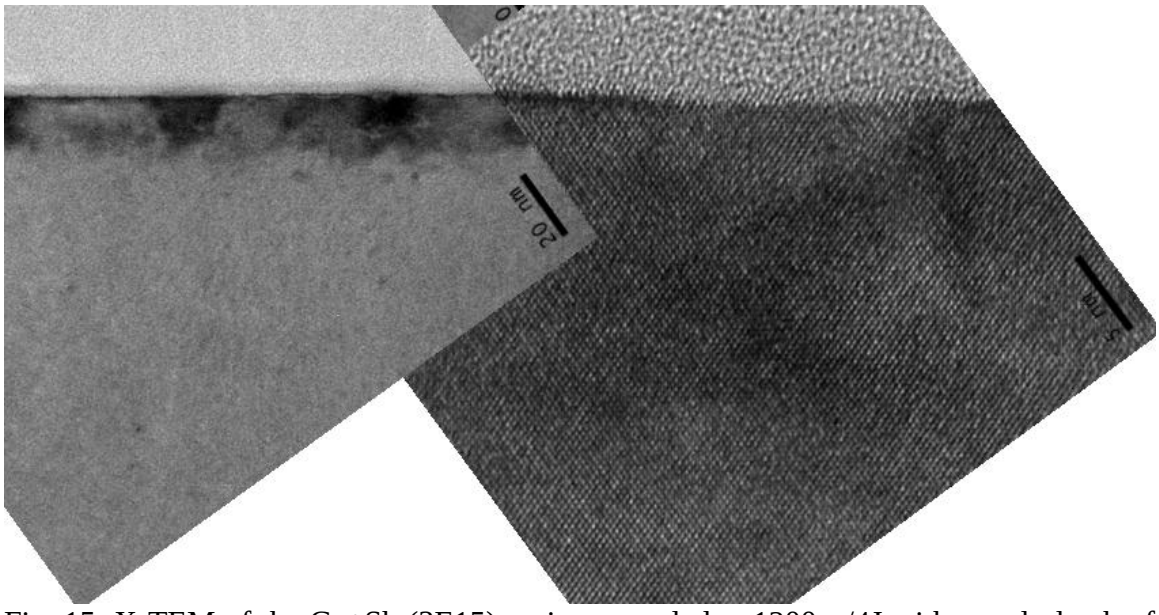

Fig. 15: X-TEM of the Ge+Sb (3E15) region annealed at 1200ns/4J with a melt depth of 25nm and TW value of 1700.

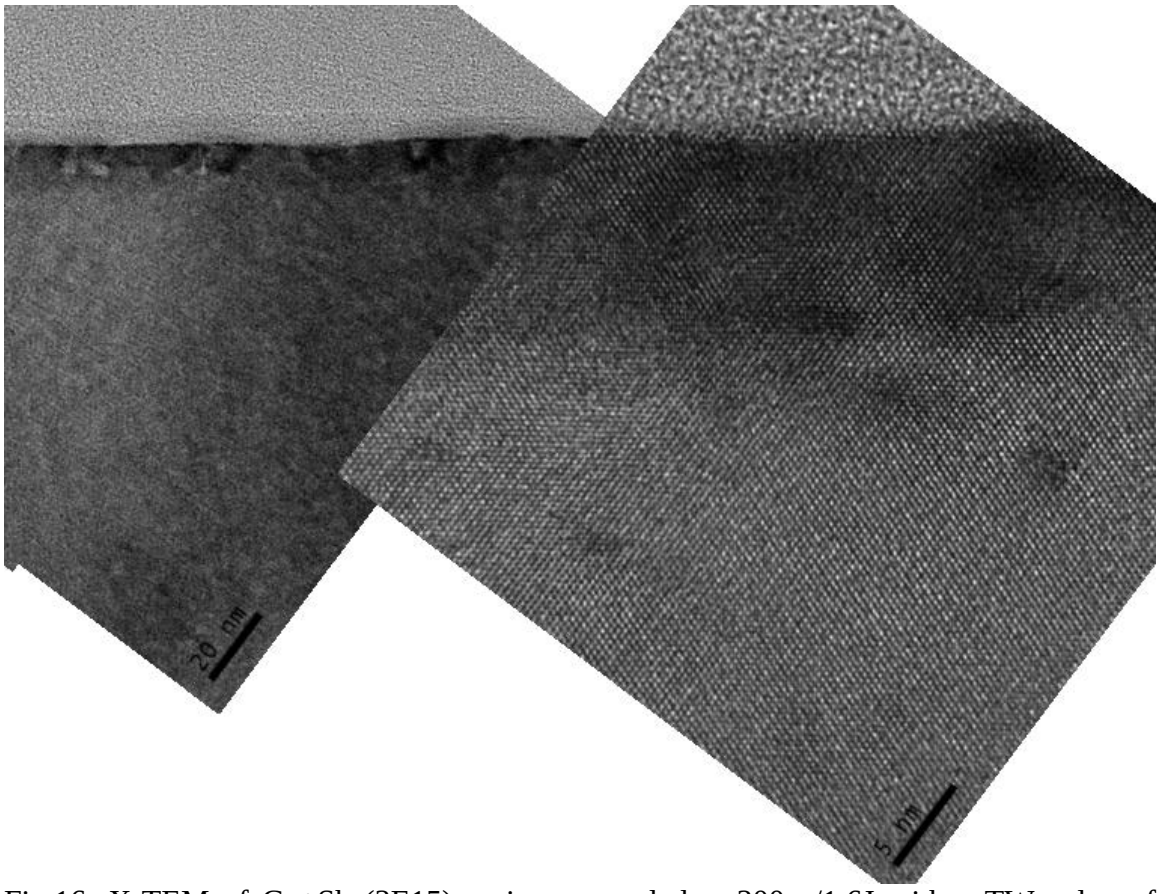

Fig.16: X-TEM of Ge+Sb (3E15) region aannealed at 300ns/1.6J with a TW value of 1600 and observved melt depth of <10nm.

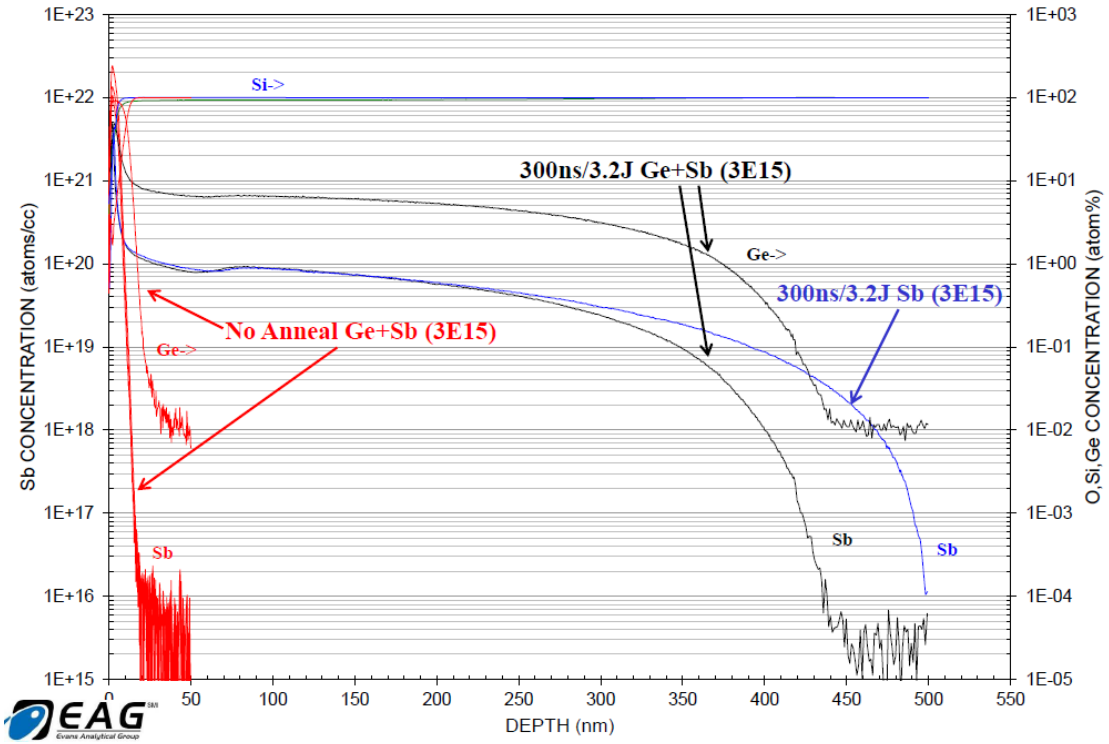

Fig.17: SIMS profile comparison for 300ns laser anneal at 3.2J, melt depth of 400nm for Ge+Sb region while Sb only region melt depth of 490nm.

The unannealed lower dose Ge+Sb (3E13/cm^2) SIMS results are shown in Fig. 18 below in direct comparison to the higher dose Ge+Sb (3E15/cm^2) implanted wafer. This time the Sb peak level is only 1.8E20/cm^3 (Sb areal density of 7.2E13/cm^2) with junction depth of 8.5nm and the Ge implant level only reached 80% for the same 5E16/cm^2 implant dose and a shift in Ge depth profile of ~3.5nm while the Sb profile shift in junction depth was 4nm. The Ge areal density was 2.6E16/cm^2 so 40% less Ge than the 4.4E16/cm^2 for the higher dose Sb wafer. This suggests that an amorphous Si surface caused by the high dose Sb implant prevents Ge implant surface sputtering while a crystalline Si surface results in Ge implant surface sputtering of about 3.5-4.0nm limiting Ge surface content to <80% and this would explain plasma Ge implantation surface sputter limit of 55% reported last year by Borland (7). The after laser anneal SIMS profiles are shown in Figs.19&20 below. In Fig.19, the 600ns/2J laser anneal condition results in a melt depth of only 9nm based on the clear O-SIMS pile-up at 8nm and Sb-SIMS liquid phase diffusion and x_j of 10nm. The Ge-SIMS profile was also 1nm deeper. Next the 1200ns/4J laser anneal resulted in deeper O-SIMS melt to 12nm, deeper Ge-SIMS by 5nm but same Sb x_j with a box-like profile level of 6E18/cm^3. The 300ns/1.6J laser anneal melt depth was 14nm with Sb x_j at 12nm and slightly deeper Ge. No 4PP Rs value could be measured on any of these samples (see Fig.9). However, 4PP Rs measurements on the deeper melt samples showed up to 100% Sb dopant activation in Fig.9. In Fig.20, the 600ns/4J laser anneal results in a Ge melt depth of 250nm and a box-like profile for both Ge and Sb by SIMS. The Ge level is between 2-4% (Ge areal density of 2.3E16/cm^2) and the Sb level is 1.3E18/cm^3 (Sb areal density of 2.2E13/cm^2). A 300ns/3.2J laser anneal results in a Ge melt depth of 450nm with a surface Ge level of 1.5% and Sb 1E18/cm^3 as shown in Fig.20. Note the Ge melt depth in Fig.17 for the same laser anneal condition was 400nm and Ge level was 7%, >4.5x higher so clearly Ge surface sputter limited the Ge incorporation level with the low dose Sb at 3E13/cm^2.

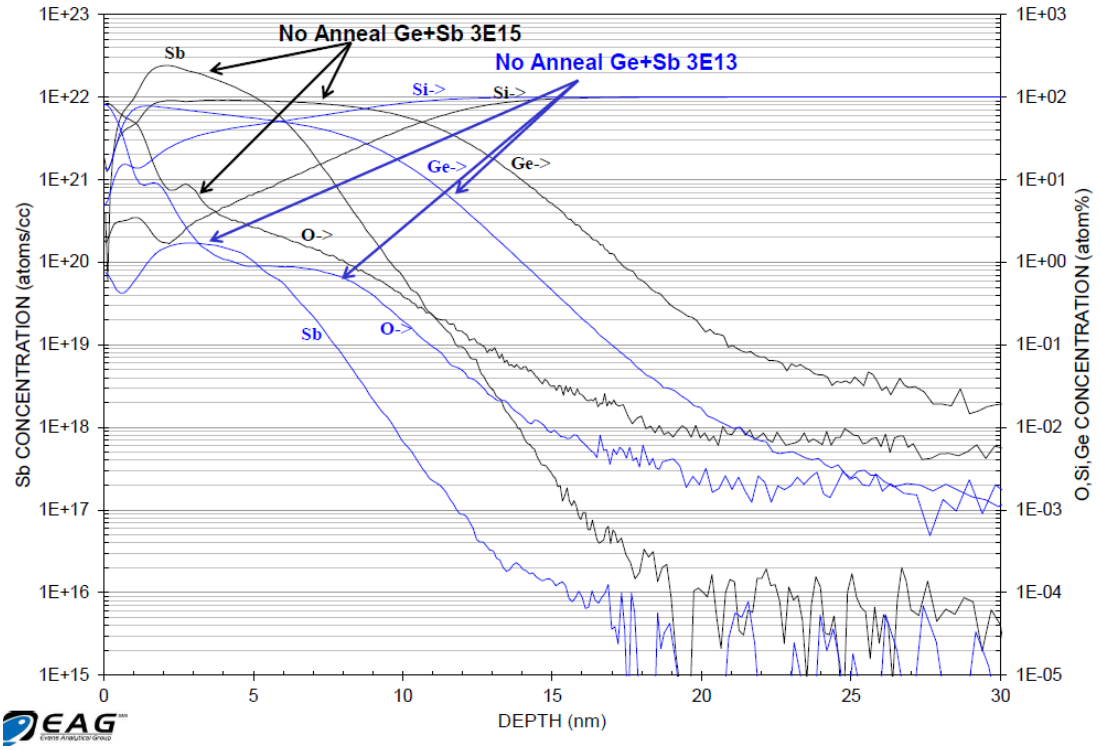

Fig.18: SIMS comparison of no anneal regions for Ge+Sb 3E13 and 3E15.

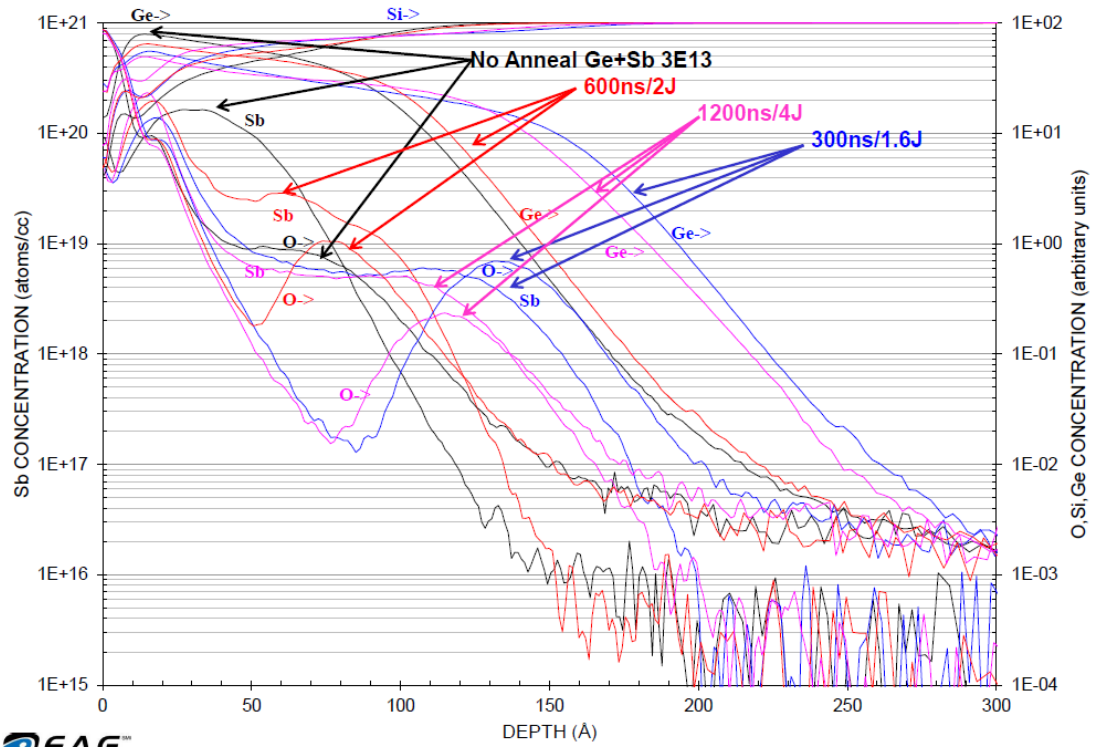

Fig.19: SIMS profile comparison for Ge(5E16)+Sb(3E13) at a) no anneal, b) 1200ns at 4J, c) 600ns at 2J and d) 300ns at 1.6J.

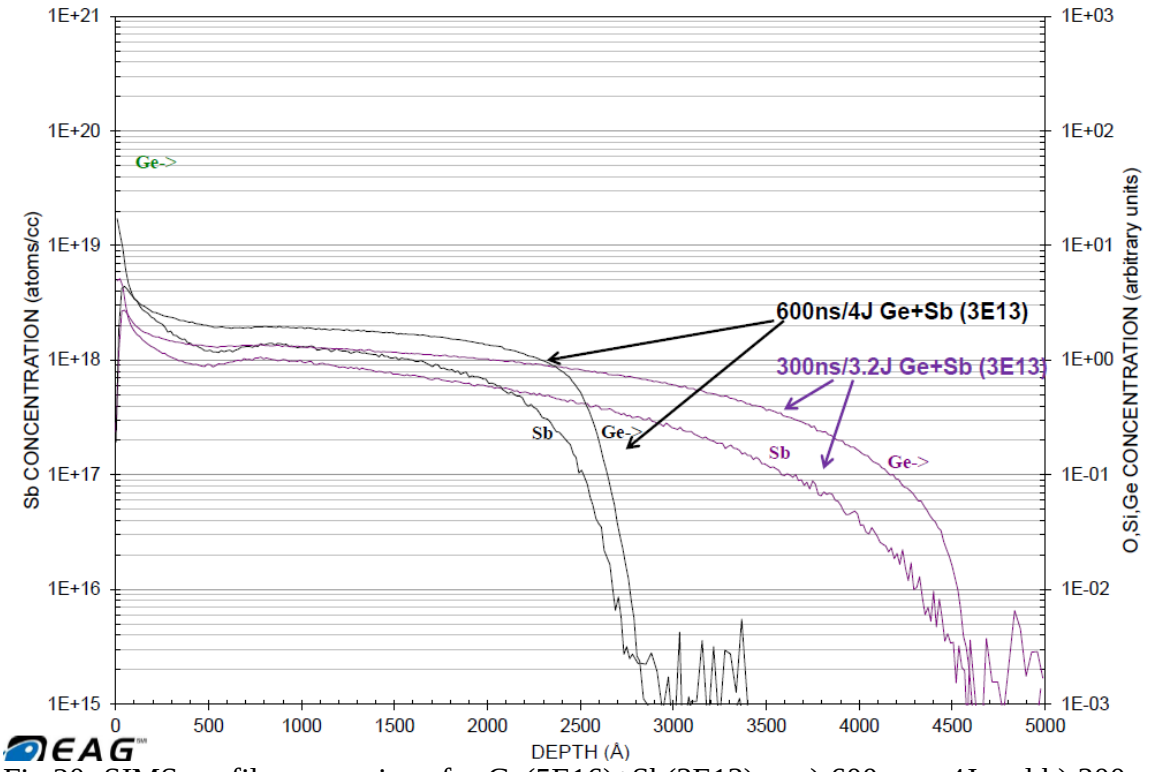

Fig.20: SIMS profile comparison for Ge(5E16)+Sb(3E13) at a) 600ns at 4J and b) 300ns at 3.2J.

Fig.21 shows the X-TEM for the 1200ns/4J SIMS case in Fig.19. The Ge melt depth was 13nm and TW was 1100 suggesting complete LPE of the residual Ge implant

damage. Fig.22 shows the X-TEM for the 300ns/1.6J case with the Ge melt dapth of 15nm and TW value of 1100. Fig.23 is a side by side X-TEM comparison of the Sb+Ge implanted regions with the 3E15/cm^2 and 3E13/cm^2 Sb doses after the various laser annealing conditions, the ←→ shows the same scale of 20nm for all 5 X-TEM micrographs. Only in Fig.23b for the 300ns/1.6J laser condition was the melt depth <9nm too shallow resulting in some regions of defects and Ge-poly by LPE.

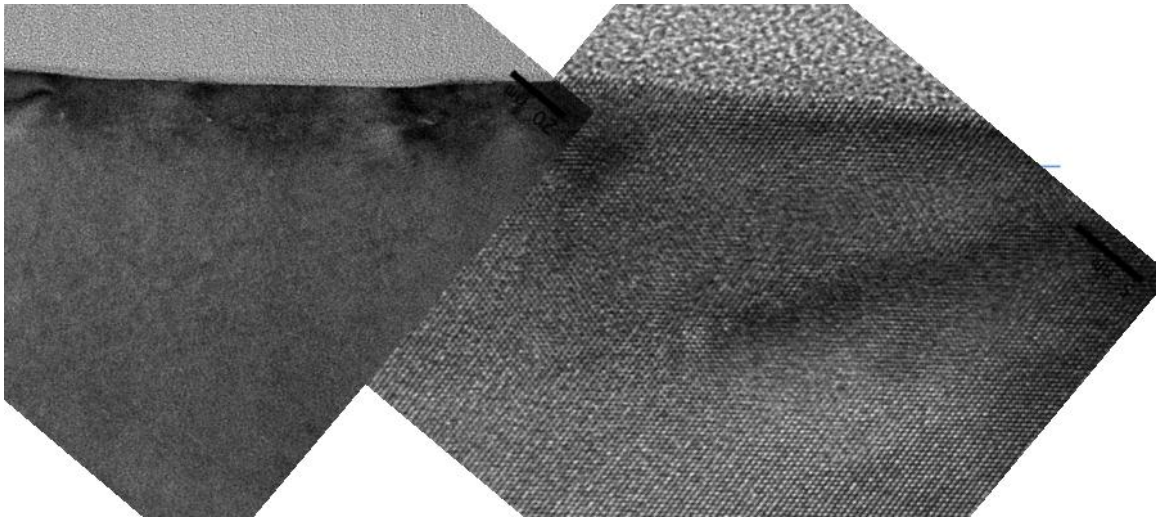

Fig.21: X-TEM of Ge+Sb (3E13) region aannealed at 1200ns/4J with a TW value of 1100 and observved melt depth of 13nm.

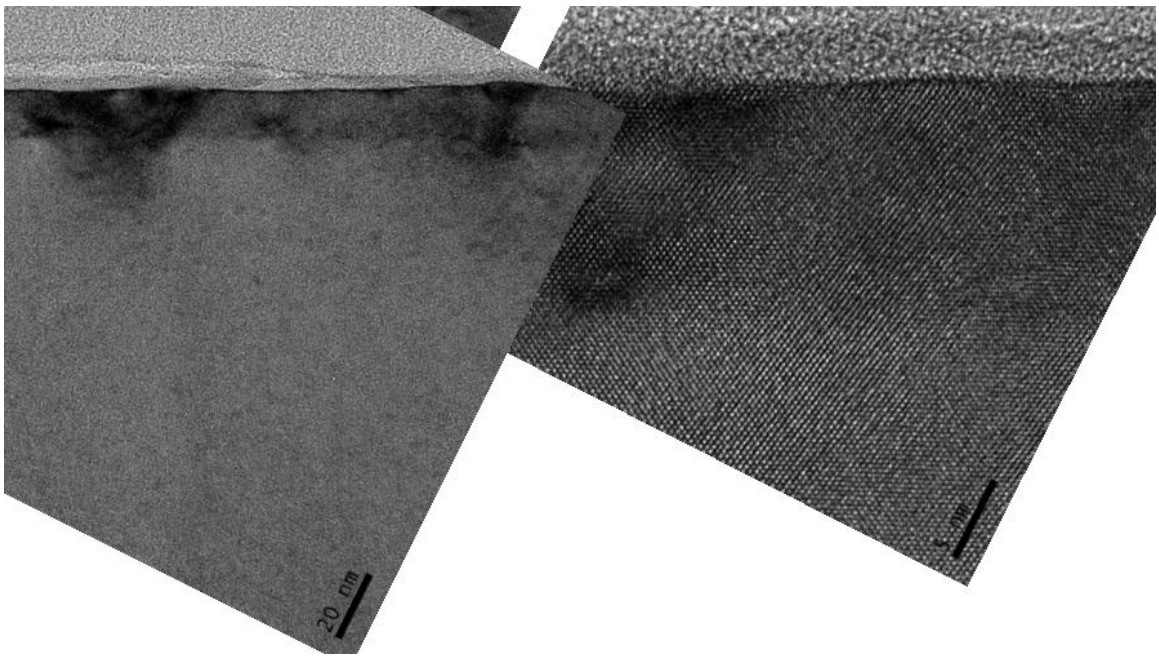

Fig.22: X-TEM of Ge+Sb (3E13) region aannealed at 300ns/1.6J with a TW value of 1100 and observved melt depth of 14nm.

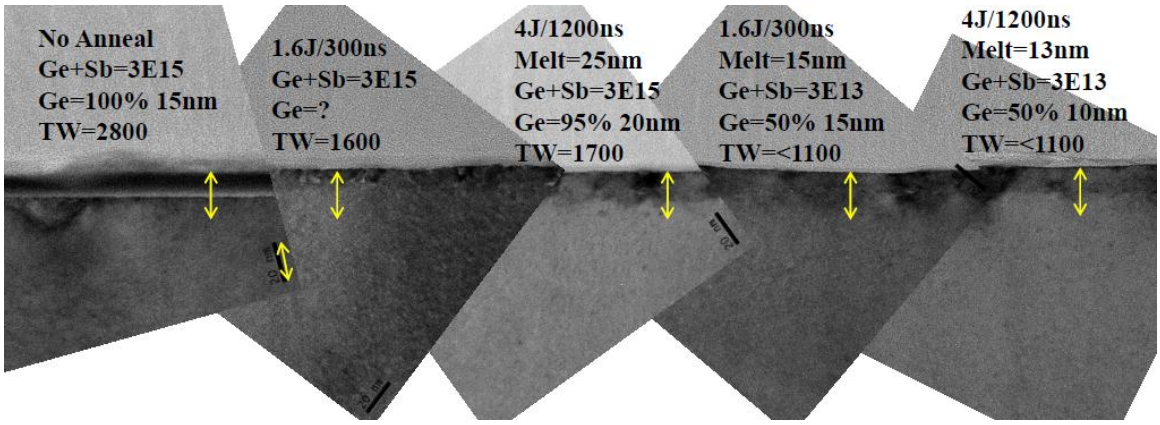

(a) (b) (c) (d) (e)

Fig.23: X-TEM comparison for the Ge+Sb at 3E15/cm^2 and 3E13/cm^2 for various laser anneals.

Differential Hall Analysis for Carrier Concentration and Mobility Measurements

Carrier concentration (electrically active Sb dopant) and electron mobility was measured by CAOT/DHE (continuous anodic oxidation technique/differential Hall effect) method by Active Layer Parametrics. Fig.24 shows the carrier concentration depth profile after laser annealing at 600ns/4J. For the Ge+Sb 3E13/cm^2 the activated carrier level was 2-4E18/cm^3 and for the Ge+Sb 3E15/cm^2 the activated carrier level was 2E20/cm^3 which is above the Sb solid solubility limit in Si of 6.8E19/cm^3. Since the carrier concentration is calculated from the resistivity, the lower resistivity value maybe due to the higher mobility from the higher Ge content. Fig.25 shows the DHE determined electrically activated concentration versus Sb and Sb+Ge implant and laser annealing conditions. The high Rs values shown in Fig.8&14 agree with the DHE activated concentration levels in Fig.25. Fig.26 shows the electron mobility values, the mobility for the Ge+Sb 3E15/cm^2 was 70cm^2/V-s dropping to 48cm^2/V-s at the surface and this is what is expected for nSi at 2E20/cm^3 (72cm^2/V-s) and not nGe which should be 110cm^2/V-s. The Ge+Sb 3E13/cm^2 was 70-120cm^2/V-s peaking at the surface at 200cm^2/V-s, this is higher than what is expected for nSi at 2-4E18/cm^3 which should be 150cm^2/V-s and nGe should be 500cm^2/V-s. Fig. 27 shows the DHE determined electron mobility for the versus Sb and Sb+Ge implant and laser annealing conditions along with the ideal mobility values for pure Ge and Si at these doping levels for comparison. For the 3E15/cm^2 Sb conditions adding the high dose Ge implant actually resulted in lower electron mobility and shallower melt depth so the lower mobility values in Fig.27 are opposite to what we expected requiring further investigation, possibly more residual implant damage when using Sb implant dopant or due to the high O areal density of 1.0E16/cm^2 shown in Fig.13.

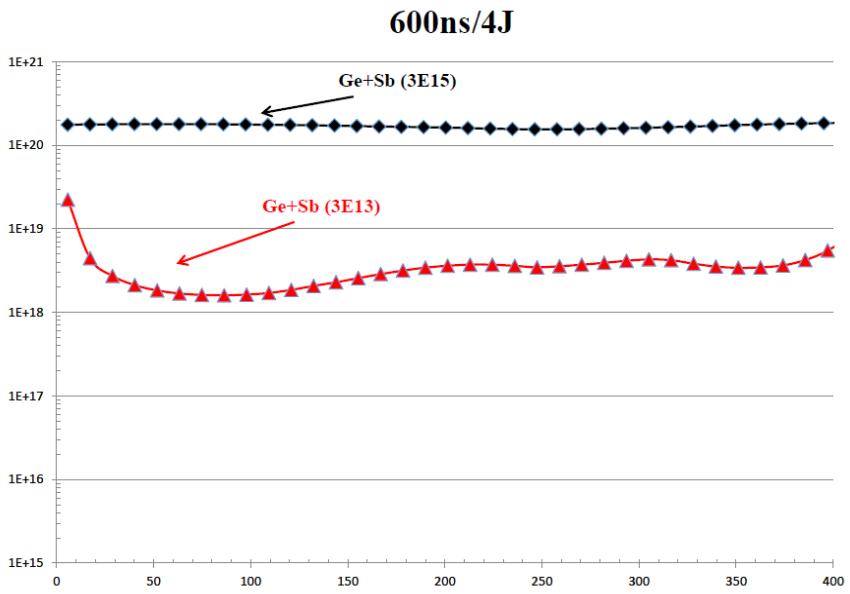

Fig. 24: Carrier concentration depth profile comparison for Ge+Sb 3E13/cm^2 and 3E15/cm^2 laser annealed at 600ns 4J/cm^2.

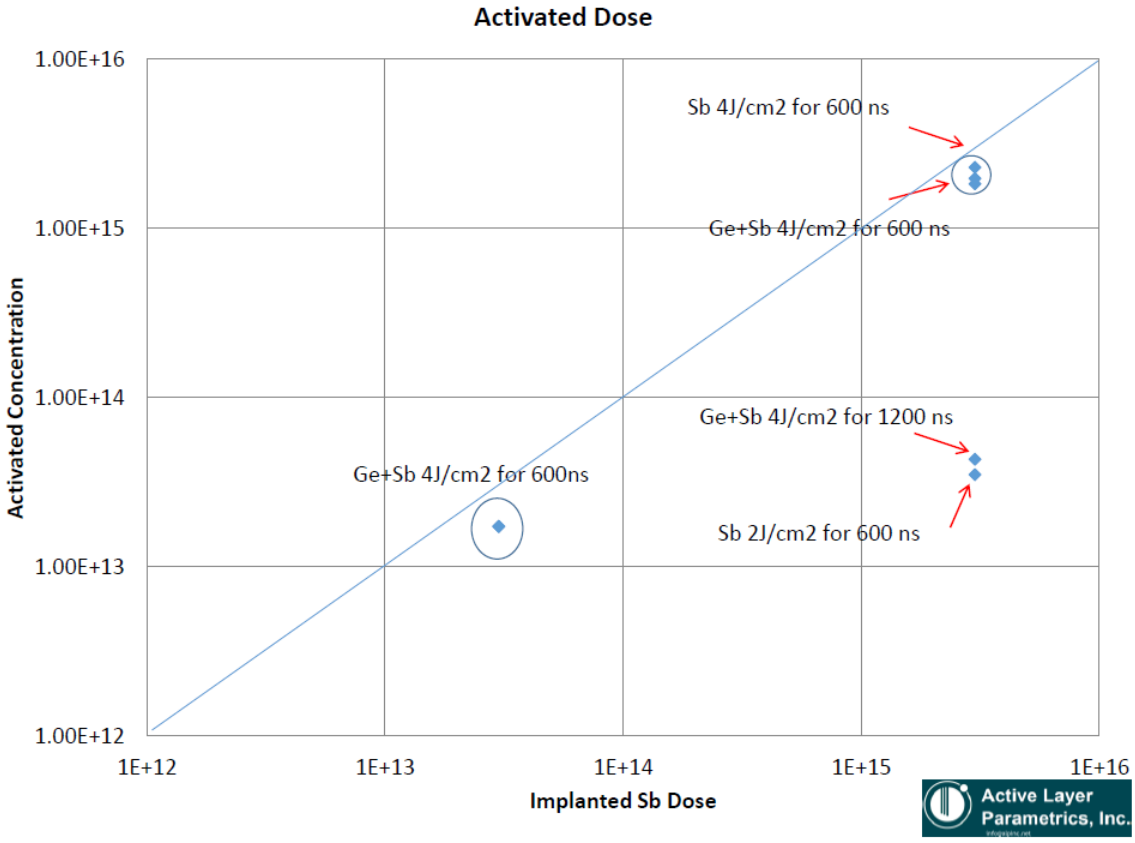

Fig.25: DHE determined Sb activated concentration for the various Sb and Sb+Ge implant and annealing conditions.

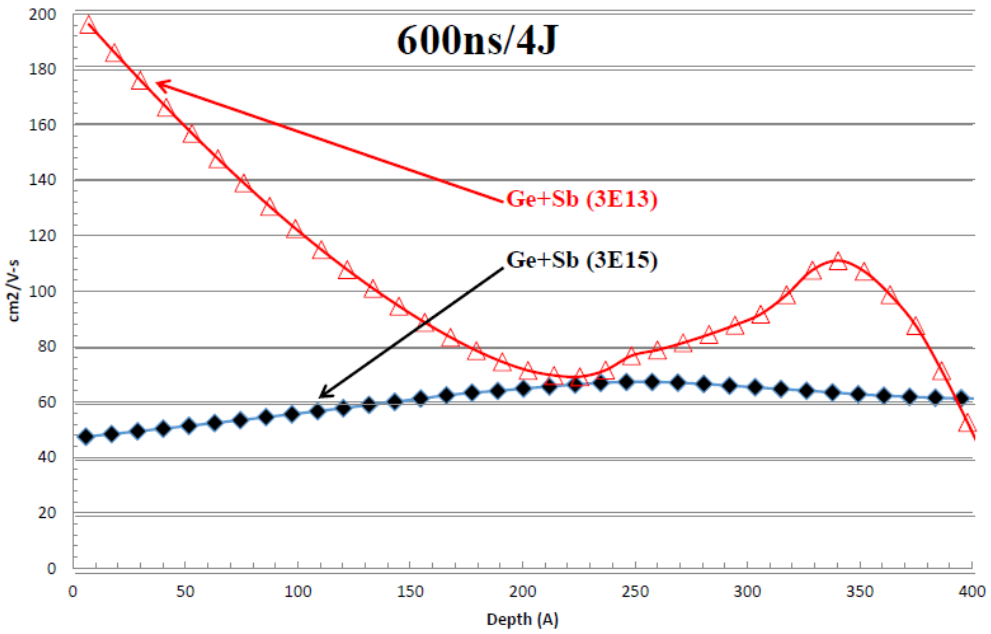

Fig.26: Electron mobility depth profile comparison for Ge+Sb 3E13/cm^2 and 3E15/cm^2 laser annealed at 600ns 4J/cm^2.

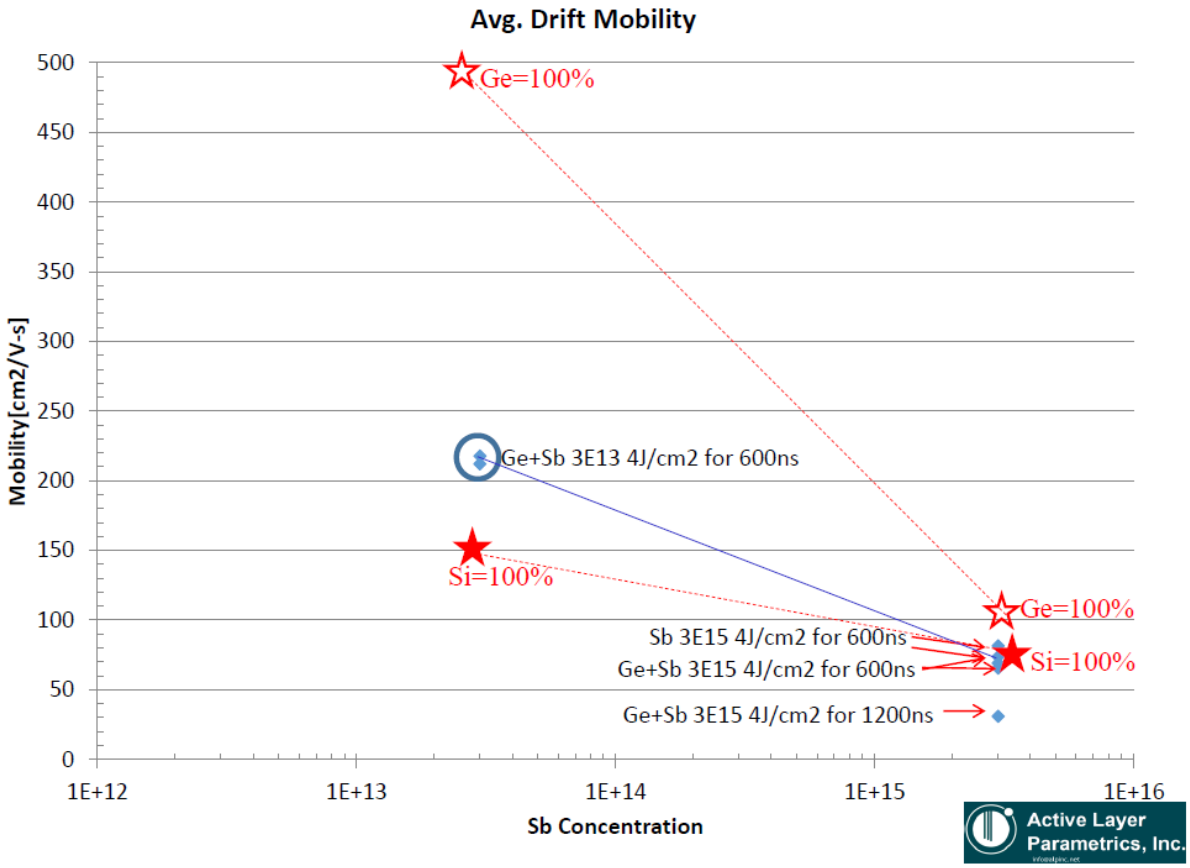

Fig.27: DHE determined Sb electron mobility for the various Sb and Sb+Ge implant and annealing conditions.

Summary

We investigated using Ge implantation in a high current beam-line implanter at 5E16/cm^2 dose and achieved 7.0nm of amorphous Ge deposition by a method called dose controlled deposition (DCD). We did notice Ge surface dose loss or sputter limited as reported with Ge plasma implantation if the Si surface was crystalline and not when it was amorphous. By optimizing the laser annealing conditions we could controll the Ge melt depths in the 9-25nm range for 50-95% surface Ge content by liquid phase epitaxial regrowth (LPE). Ion implantation produces extremely uniform and localized regions of Ge and laser melt realizes complete implant damage annealing by LPE. We used Sb for n-type implanted dopants and recommend investigating P and As and combinations next for higher dopant activation as reported Borland (5) and to see what differences dopant species may have on electron mobility enhancement in Ge.

References

1. J. Borland, IEEE RTP-2009, paper 7, page 59.
2. J. Borland et al., ECS Oct 2004 meeting, PV 2004-07, p.769.
3. J. Borland et al., Solid State Technology, July 2005, page 45.
4. J. Borland et al., US Patent #7,259,036 Aug 2007.
5. J. Borland and P. Konkola, IIT-2014 paper to be published, June 30, 2014.
6. S. Wuu et al., IEDM-2010, paper 14.1.
7. J. Borland et al., IWJT-2013 meeting, paper S4-4, page 49.
8. J. Borland et al., IEEE-PVSC, June 2012, paper 626.